Geochemistry of ultramafic xenoliths in Cenozoic alkali basalts from Jiangsu province, eastern China and their geological implication

Shao-Wei Huang[1], Yung-Tan Lee[1,2,*], Ju-Chin Chen[1], Kung-Suan Ho[3], Meng-Lung Lin[2], Yen-Tsui Hu[4] and Ren-Yi Huang[5]

[1]*Institute of Oceanography, National Taiwan University, Taipei 106, Taiwan.*
[2]*Department of Tourism, Aletheia University, Tamsui 25103, Taiwan.*
[3]*National Museum of Natural Science, Taichung 404, Taiwan.*
[4]*Sinotech Engineering Consultants Inc., Taipei 114, Taiwan.*
[5]*Department of Leisure Business Management, DeLin Institute of Technology, Taipei 236, Taiwan.*
[*]*Corresponding author. e-mail: au4300@mail.au.edu.tw*

Twelve ultramafic xenoliths in Cenozoic alkali basalts from Jiangsu province, eastern China have been analyzed for major, trace, Sr–Nd isotopic composition and mineral chemical compositions and the origin of these ultramafic xenoliths is discussed based on the geochemical constraints. Based on classification norms, the ultramafic xenoliths in the present study belong to type I xenolith. The Fo-values of the ultramafic xenoliths range from 90.18 to 92.18. The ultramafic xenoliths have higher MgO content, but lower Al_2O_3, TiO_2, CaO and Na_2O contents than those of primitive mantle, indicating that they represent residues formed by different degrees of partial melting from the upper mantle. The enrichment of Rb, Ba, U, Nb, K, La, Ce, Sr, P and Zr of ultramafic xenoliths found in Jiangsu province, eastern China may be related to the CO_2–H_2O-fluids metasomatism. On the basis of Sr–Nd isotopic ratios, we suggest that the lithospheric mantle beneath the study area mostly belongs to depleted-type mantle but with slightly enriched signatures, indicating the heterogeneous characteristics in the mantle source and the influence of different degrees of fluids-metasomatism on the mantle composition. The equilibrium P–T conditions of the spinel lherzolite xenoliths are: T = 913 ∼ 1045°C, P = 13 ∼ 22 kb corresponding to depths of 45–83 km. The P–T conditions suggest that the geothermal gradient of the upper mantle beneath the study area is approximately similar to oceanic geotherm which may be caused by asthenosphere upwelling. We suggested that lithospheric mantle thinning accompanied by asthenosphere upwelling has occurred and a newly accreted and cooled asthenospheric mantle may exist beneath the study area.

1. Introduction

Most xenoliths can be used to estimate the pressures and temperatures of formation in terms of available experimental data. These temperature and pressure estimates from ultramafic xenoliths may provide important information on the thermal and dynamic evolution of their lithospheric source region. The ultramafic xenoliths found in Panshishan area, Jiangsu province (figure 1) were situated in the boundary of Yangtze Craton and southeastern edge of Sino-Korean Craton, is one of the oldest Archean continental nuclei in the world (Jahn *et al.* 1987; Jahn 1990; Liu *et al.* 1992;

Keywords. Ultramafic xenoliths; geochemistry; metasomatism; Jiangsu province.

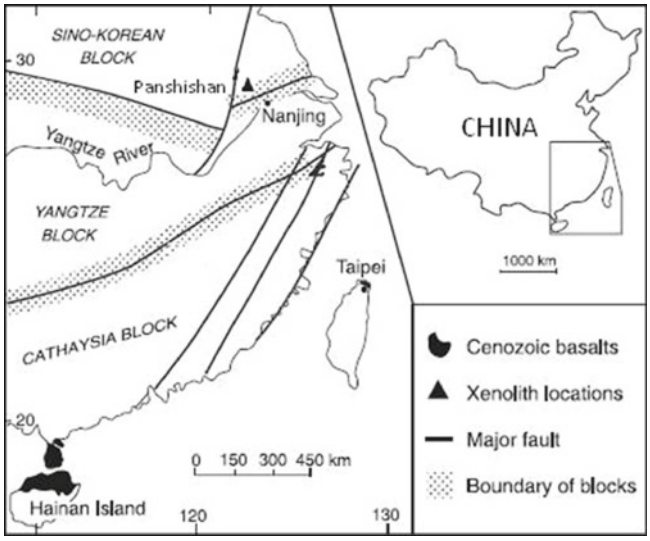

Figure 1. Sketch map of the tectonic framework and distribution of Cenozoic basaltic rocks in SE China. Three blocks are defined, from south to north: the Cathaysia, Yangtze and Sino-Korean blocks. The Panshishan sample locality of this study is shown as a triangle.

Huang *et al.* 2004). Systematic studies of eastern part of the NCC demonstrated a thinner (<80 km) and hotter lithosphere occured in the Cenozoic (Menzies *et al.* 1993; Fan *et al.* 2000). The timing, extent and mechanisms of thinning the lithospheric mantle beneath the North China Craton are yet to be fully understood (Zhang *et al.* 1998; O'Reilly *et al.* 2001; Gao *et al.* 2002; Wilde *et al.* 2003). The research of these ultramafic xenoliths in Cenozoic alkali basalts from Jiangsu province, easten China can provide new geochemical, isotope data, mineral chemistry and P–T data. The results may shed some light on the nearby North China Craton which is now accepted to lack the lithospheric roots and perhaps Jiangsu province, eastern China too joins it. The Sino-Korean Craton has preserved crustal remnants as old as 3800 Ma (Liu *et al.* 1992), and is the largest cratonic block in China, covering an area of more than 15,00,000 km^2. The Sulu ultrahigh pressure metamorphic belt caused by the collision between the Sino-Korean Craton and the Yangtze Craton in Triassic time was extrapolated as the suture of the Sino-Korean Craton and the Yangtze Craton to the east of Tanlu fault zone (Okay and Sengör 1992; Yin and Nie 1993).

Previous studies (Li 1994; Chung 1999; Huang *et al.* 2004; Ying *et al.* 2006) agree with a crustal-detachment model for the suturing of the Sino-Korean Craton and the Yangtze Craton. The model mentioned above postulated the upper crust of the Yangtze Craton was detached and thrusted northward over the Sino-Korean Craton for about 400 km, whereas the lower part of its lithospheric mantle was subducted under the Sino-Korean Craton along the subsurface suture extending eastward from Nanjing. On the basis of this model, the lower crust and the lithospheric mantle beneath the studied area may have a Sino-Korean Craton character. The Sino-Korean Craton which was extensively thinned during the Late Mesozoic and Cenozoic resulted from the replacement of old, cold and depleted lithospheric mantle by young, hot and fertile mantle (Menzies *et al.* 1993; Griffin *et al.* 1998) can be divided into the Eastern, Western Blocks and the intervening Trans-North China Orogen (TNCO) (Zhao 2001).

The lithological, geochemical, structural, metamorphic and geochronological characters are different in Eastern and Western Blocks (Zhao 2001). The spatial distribution of volcanic rocks in the study area is controlled by NNE-trending Tan-Lu fault occurred as a result of lithospheric extension. The relatively thin crust and lithosphere in eastern China may be caused by mantle upwelling which triggered partial melting of lithospheric mantle (Chung 1999; Deng *et al.* 2004; Lee *et al.* 2006). Lee *et al.* (2006) pointed out that basaltic rocks from Shandong province may be derived from partial melting of lithospheric mantle (MORB-like) involved a few EM1 components which may be produced by the recent H_2O–CO_2 fluid metasomatism.

In recent years, several authors (Xu 2001; Guo *et al.* 2003; Xu *et al.* 2004; Zhang *et al.* 2006) proposed that thinning of the lithosphere beneath the North China Craton (NCC) may have occurred since the Palaeozoic, probably due to the loss of physical integrity of the craton resulted from the Triassic collision between the NCC and the Yangtze Block. The lithospheric mantle in the western SKC is relatively old compared with that beneath the eastern SKC, which may be a mixture of old lithospheric relicts and newly accreted mantle (Xu *et al.* 2004). When compared to the MORB source (50–250 ppm), the Cenozoic lithospheric mantle of the western part of the north craton is dominated by much lower water content (Xia *et al.* 2013). The low H_2O content likely results from mantle reheating, possibly due to an upwelling asthenospheric flow during the late Mesozoic-early Cenozoic lithospheric thinning of the NCC (Xia *et al.* 2013).

In this paper, we report the major, trace elements (including rare-earth elements) and Sr–Nd isotopic composition of ultramafic xenoliths combined with the constituent mineral chemical compositions in order to deduce the origin of these ultramafic xenoliths and the geochemical characteristics of the upper mantle as well as deep geological processes beneath Jiangsu province.

2. General geological settings

The Panshishan area, Jiangsu province, eastern China (figure 2) is tectonically located in the boundary of Yangtze Craton and southeastern edge of Sino-Korean Craton, is one of the oldest Archean continental nuclei in the world (Jahn *et al.* 1987; Jahn 1990; Liu *et al.* 1992; Huang *et al.* 2004).

NE China can be divided into two main tectonic domains: the south Precambrian Sino-Korean Craton and the north Paleozoic Xing'an-Mongolian fold belt (Chen *et al.* 2003). Menzies and Xu (1998) suggested that the Archean lithostratigraphy beneath Sino-Korean Craton had survived which was characterized by a cold, thick, refractory mantle keel in early Palaeozoic based on geochronological and geochemical evidences of kimberlite-born xenoliths and diamonds from Shandong and Liaoning provinces. On the basis of seismic tomography, Liu *et al.* (1992) pointed out that the lithosphere in the eastern part of the NCC is <80 km thick and even thinner around the Bo Sea. Zhang (2005) based on olivine xenocrysts with clear compositional zonations in early Cretaceous Fangcheng basalts erupted in Luxi region of Shandong province, north China concluded that mantle-melt reaction was significant in the Mesozoic lithospheric mantle beneath the southeastern portion of the Sino-Korean Craton which he considered to be responsible for the replacement of lithospheric mantle from the Paleozoic refractory peridotitic mantle to the late Mesozoic fertile and enriched mantle. During the Mesozoic and Cenozoic, the tectonic evolution of China was closely related to the complex interaction of the Eurasian, Indian and Pacific plates. The collision between the NCC and adjacent areas may have been associated with the reactivation of the Tancheng-Lujiang (Tan-Lu) fault extending about 2000 km. The Tan-Lu system is regarded as a major transcurrent intracontinental fault zone with over 700 km of sinistral displacement and it may have taken place in Cretaceous time (Xu *et al.* 1987; Xu 1993; Xu and Zhu 1994).

Cenozoic basalts are widely distributed along the eastern China from north of Heilongjiang province to south of Hainan island, and South China Sea (Zou *et al.* 2000). The Cenozoic volcanic rocks from Anhui–Jiangsu provinces are spread over an area of more than 2000 km^2 in eastern Anhui and western Jiangsu. The spatial distribution of volcanic rocks in this region is controlled by the NNE-trending Tan-Lu fault and its adjacent NW-trending basins and faults which can be divided into three periods (Chen and Peng 1985; Dostal *et al.* 1991): (A) volcanic rocks of 1st period – non-marine fissure eruption of Paleogene located in the central and eastern parts of the Subei basin are mainly tholeiites, olivine tholeiites and alkali basalts intercalated with Paleocene, Eocene and Oligocene sedimentary sequences. (B) volcanic rocks of 2nd period – mainly lava flows and pyroclastic rocks of Pliocene lie on the top of fossiliferous sediments of Miocene and early Pliocene age. The Pliocene volcanic rocks located in the southwestern part of the Subei basin include alkali olivine basalts and related rocks, covering an area of about 1500 km^2. (C) volcanic rocks of 3 rd period – the eruption process of this period occurred in Pleistocene and produced basanites and olivine nephelinites with abundant peridotite xenoliths and megacrysts.

The xenoliths of this study generally range from 10 to 20 cm in diameter and are green in their appearance which contain pale green

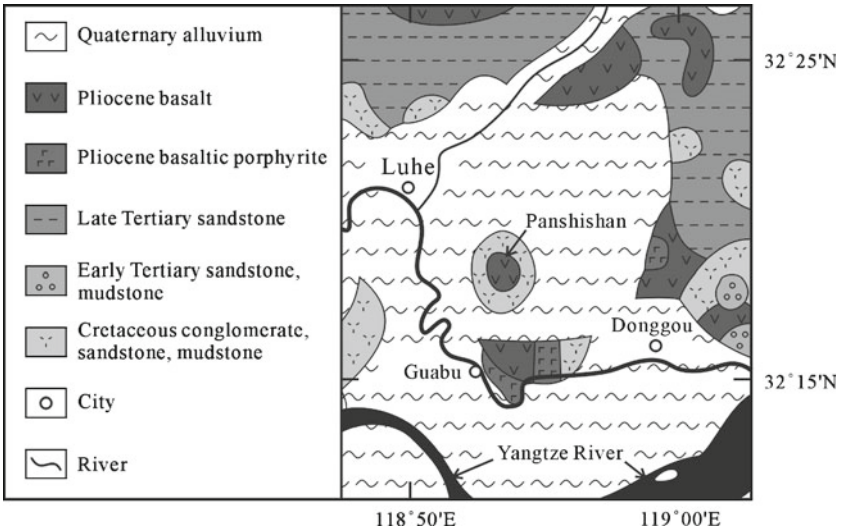

Figure 2. Geological map showing the sampling location of Panshishan in the Jiangsu province, eastern China.

Table 1. *The chemical compositions of olivine in the ultramafic xenoliths from the Panshishan area, Jiangsu province.*

	JMX1-OL	JMX2-OL	JMX3-OL	JMX4-OL	JMX5-OL	JMX6-OL	JMX7-OL	JMX8-OL	JMX9-OL	JMX10-OL	JMX11-OL	JMX12-OL
SiO_2 (wt%)	40.98	41.49	41.26	41.06	38.43	38.28	39.81	40.78	40.00	40.54	41.36	40.79
TiO_2	0.02	0.03	0.01	0.02	0.02	0.00	0.00	0.01	0.01	0.01	0.01	0.02
Al_2O_3	0.02	0.01	0.00	0.09	0.00	0.00	0.03	0.04	0.03	0.03	0.00	0.00
Cr_2O_3	0.02	0.03	0.02	0.02	0.03	0.02	0.02	0.04	0.02	0.01	0.03	0.01
ΣFeO	8.94	7.85	7.93	9.95	9.29	9.12	9.32	8.13	9.87	9.75	7.94	9.43
MnO	0.14	0.12	0.10	0.17	0.14	0.14	0.14	0.14	0.24	0.16	0.13	0.14
MgO	49.63	51.08	50.17	48.76	52.03	52.16	50.27	50.46	49.49	49.37	50.60	49.42
CaO	0.05	0.05	0.05	0.04	0.04	0.08	0.05	0.08	0.06	0.06	0.06	0.02
Na_2O	0.01	0.00	0.01	0.01	0.00	0.00	0.01	0.00	0.02	0.01	0.00	0.01
K_2O	0.01	0.00	0.00	0.04	0.01	0.00	0.00	0.01	0.02	0.00	0.00	0.01
Total	99.80	100.66	99.55	100.16	99.98	99.79	99.65	99.68	99.78	99.94	100.12	99.84
Number of cations on the basis of 4 Oxygens												
Si	1.000	0.998	1.003	0.998	0.946	0.942	0.977	0.993	0.99	0.991	1.000	0.996
Fe	0.179	0.156	0.159	0.170	0.188	0.185	0.186	0.165	0.198	0.197	0.158	0.193
Mg	1.800	1.832	1.819	1.744	1.903	1.916	1.839	1.834	1.802	1.800	1.825	1.800
Mn	0.003	0.002	0.002	0.004	0.003	0.003	0.003	0.003	0.004	0.003	0.003	0.003
Ca	0.002	0.001	0.002	0.001	0.001	0.002	0.001	0.002	0.002	0.002	0.002	0.001
Fo	90.58	92.18	91.99	90.30	91.02	91.20	90.74	91.85	90.39	90.18	92.05	90.48
Fa	9.42	7.82	8.01	9.70	8.98	8.80	9.26	8.15	9.61	9.82	7.95	9.52

Table 2. *The chemical compositions of orthopyroxene in the ultramafic xenoliths from the Panshishan area, Jiangsu province.*

	JMX1-OPX	JMX2-OPX	JMX3-OPX	JMX4-OPX	JMX5-OPX	JMX6-OPX	JMX7-OPX	JMX8-OPX	JMX9-OPX	JMX10-OPX	JMX11-OPX	JMX12-OPX
SiO_2 (wt%)	56.29	56.00	56.67	55.43	53.14	55.53	54.79	56.22	54.40	55.65	56.28	55.09
TiO_2	0.02	0.06	0.06	0.14	0.10	0.09	0.11	0.02	0.13	0.10	0.05	0.08
Al_2O_3	2.25	2.48	2.38	4.65	3.93	3.76	4.41	3.99	4.75	4.56	2.68	3.69
Cr_2O_3	0.39	0.57	0.54	0.35	0.30	0.54	0.43	0.58	0.37	0.30	0.60	0.35
ΣFeO	5.81	4.99	4.97	6.36	6.02	6.07	5.76	5.22	6.23	6.20	4.88	6.13
MnO	0.15	0.13	0.11	0.14	0.13	0.15	0.15	0.13	0.16	0.15	0.14	0.14
MgO	34.35	34.83	34.39	32.35	35.59	32.77	33.24	33.01	32.96	31.96	34.13	33.91
CaO	0.49	0.64	0.62	0.62	0.58	0.78	0.67	0.89	0.61	0.59	0.62	0.44
Na_2O	0.00	0.11	0.17	0.09	0.11	0.17	0.09	0.15	0.12	0.12	0.15	0.04
K_2O	0.01	0.01	0.00	0.01	0.00	0.00	0.00	0.01	0.01	0.00	0.00	0.01
Total	99.75	99.81	99.91	100.15	99.89	99.86	99.66	100.21	99.74	99.62	99.53	99.89
Number of cations on the basis of 6 Oxygens												
Mol %												
En	90.41	91.38	91.37	88.92	90.08	89.14	89.878	90.19	89.26	89.05	91.39	89.98
Fs	8.66	7.41	7.45	9.86	8.84	9.34	8.82	8.07	9.55	9.77	7.42	9.18
Wo	0.93	1.21	1.18	1.23	1.09	1.53	1.30	1.75	1.19	1.18	1.19	0.84
Mg.no.	90.97	93.38	91.44	88.92	95.84	89.14	90.85	90.19	90.95	89.05	91.39	91.94

Table 3. *The chemical compositions of clinopyroxene in the ultramafic xenoliths from the Panshishan area, Jiangsu province.*

	JMX1-CPX	JMX2-CPX	JMX3-CPX	JMX4-CPX	JMX5-CPX	JMX6-CPX	JMX7-CPX	JMX8-CPX	JMX9-CPX	JMX10-CPX	JMX11-CPX	JMX12-CPX
SiO_2 (wt%)	53.86	53.36	53.97	52.64	52.08	51.26	52.39	53.61	51.96	51.94	51.69	51.15
TiO_2	0.11	0.35	0.21	0.52	0.50	0.29	0.40	0.10	0.51	0.46	0.22	0.46
Al_2O_3	2.14	3.32	4.37	7.06	5.96	5.49	6.50	5.39	7.20	7.55	4.75	6.15
Cr_2O_3	0.69	1.48	1.51	0.75	0.73	1.18	0.95	1.14	0.85	0.79	1.60	0.99
ΣFeO	1.99	2.33	2.25	2.71	2.58	2.86	2.49	2.43	2.66	2.57	2.24	2.28
MnO	0.05	0.07	0.08	0.10	0.09	0.11	0.09	0.09	0.09	0.10	0.10	0.09
MgO	17.45	17.17	15.89	14.75	15.67	17.25	15.38	16.49	14.34	14.42	17.60	15.62
CaO	23.49	20.05	18.68	20.08	19.97	19.01	19.98	18.69	19.68	19.83	19.07	21.40
Na_2O	0.32	1.51	2.57	2.08	2.52	2.34	2.05	1.84	2.48	1.83	2.48	1.79
Total	100.11	99.65	99.53	100.70	100.11	99.81	100.23	99.79	99.78	99.50	99.75	99.93
Number of cations on the basis of 6 Oxygens												
Mol %												
En	49.10	50.34	49.56	47.48	50.39	52.52	47.40	50.06	47.09	47.25	53.28	48.31
Fs	2.57	2.63	4.01	4.00	3.46	4.22	3.91	4.00	4.25	4.70	3.34	3.17
Wo	48.33	47.02	46.43	48.52	46.15	43.26	48.69	45.94	48.66	48.05	43.39	48.52
Mg.no.	95.04	92.37	92.51	92.26	92.37	92.56	91.81	91.99	91.72	90.96	93.13	93.12

Table 4. *The chemical compositions of spinel in the ultramafic xenoliths from the Panshishan area, Jiangsu province.*

	JMX1-SP	JMX2-SP	JMX3-SP	JMX4-SP	JMX5-SP	JMX6-SP	JMX7-SP	JMX8-SP	JMX9-SP	JMX10-SP	JMX11-SP	JMX12-SP
SiO_2 (wt%)	0.06	0.05	0.07	0.08	0.08	0.07	0.08	0.10	0.08	0.08	0.11	0.08
TiO_2	0.08	0.19	0.20	0.13	0.11	0.21	0.14	0.22	0.15	0.10	0.19	0.04
Al_2O_3	35.61	33.41	32.77	57.58	58.98	46.79	53.19	45.39	55.74	57.84	33.78	55.98
Cr_2O_3	32.84	35.35	35.89	9.83	9.61	21.16	14.33	22.05	10.82	9.46	34.20	11.52
ΣFeO	15.03	12.90	13.02	10.76	10.26	12.98	10.59	11.74	11.01	10.60	12.92	10.31
MnO	0.10	0.08	0.07	0.09	0.09	0.09	0.07	0.07	0.09	0.07	0.07	0.06
MgO	16.24	17.50	17.29	20.89	20.65	18.52	20.90	20.14	21.28	21.43	17.84	21.26
CaO	0.04	0.00	0.02	0.01	0.02	0.01	0.01	0.02	0.00	0.00	0.01	0.01
NiO	0.21	0.20	0.18	0.36	0.36	0.33	0.35	0.24	0.39	0.39	0.23	0.35
Total	100.22	99.69	99.50	99.73	100.16	100.16	99.66	99.95	99.56	99.97	99.36	99.62
Number of cations on the basis of 32 Oxygens												
Mol %												
$MgAl_2O_4$	60.15	56.81	56.03	80.73	79.30	75.14	82.04	72.63	82.69	82.31	57.42	82.35
$MgCr_2O_4$	9.21	18.44	18.72	0	0	0.05	0	8.85	0	0	19.26	0
$FeAl_2O_4$	0	0	0	0	0	0	0	0	0	0	0	0
$FeCr_2O_4$	28.01	21.89	22.44	17.39	20.11	22.76	15.48	14.82	14.15	15.22	19.74	15.28
Fe_2TiO_4	0	0	0	0	0	0	0	0	0	0	0	0
$MnFe_2O_4$	0.24	2.00	0.17	0.20	0.20	0.21	0.16	0.16	0.2	0.15	0.17	0.13
$FeFe_2O_4$	2.39	2.67	2.64	1.68	0.40	1.85	2.33	3.54	2.96	2.31	3.42	2.24

olivine, brownish orthopyroxene, bright emerald green clinopyroxene and black low spinel. They have fine- to coarse-grained porphyroclastic texture with curved cleavage.

3. Analytical methods

Twelve Jiangsu ultramafic xenoliths were selected for mineral and bulk chemical analyses. The major element compositions of four constituent phases were analyzed by a 4-spectrometer ARL-SEMQ electron microprobe at the Central Geological Survey Taipei, and corrected with the Bence and Albee correction procedures (Bence and Albee 1968). The electron beam current and accelerating voltage were usually 15 nA and 15 kV respectively, with a counting time of 20 s. Synthetic and natural minerals were utilized as standards. Analytical results of each mineral represent more than five complete point analyses of each grain, and several grains from different parts of each sample. The bulk chemical analyses of the ultramafic xenoliths in the present study have been carried out by colorimetry (Si, Al, Ti, P), atomic absorption (Fe, Mg, Ca, Na, K, Mn, Cr, Ni) and inductively coupled plasma mass spectrometry (Ba, Co, Cu, Hf, Li, Nb, Pb, Rb, Sc, Sr, Th, U, V, Y, Zn, Zr and REEs) at the National Taiwan and Tsing-Hua Universities.

The calibration curves were constructed using USGS standard rocks BHVO-1, AGV-1, BCR-1, W-2, G2 and NBS standard rock basalt. The precision of the analyses in the present study is estimated to be around ±2% for colorimetric and atomic absorption methods and better than ±5% for all ICP-MS analyses.

Seven ultramafic xenoliths (JMX1, JMX2, JMX3, JMX6, JMX7, JMX10, and JMX11) were selected for Sr and Nd isotopic composition analyses. Isotopic compositions of the Sr and Nd were measured using a Finnigan MAT 262 mass spectrometer at National Cheng Kung University followed the procedures of Smith and Huang (1997). Precision of Nd and Sr isotopic compositions is better than ±0.000010 (2σ).

4. Mineral composition of ultramafic xenoliths

The ultramafic xenoliths found in Cenozoic basaltic rocks from the Panshishan area of Jiangsu province are mainly spinel-lherzolites. The ultramafic xenoliths found in the study area are mainly spinel-lherzolites. Most of them consist of olivine, clinopyroxene, orthopyroxene and spinel. The clinopyroxenes in the ultramafic xenoliths are generally interstitial and smaller in size than coexisting olivine and orthopyroxene. Spinels form a common accessory phase (2–5 vol.%) in ultramafic xenoliths. Under microscopic observation, the spinel-lherzolites have porphyroclastic texture with curved cleavage and wavy extinction.

The results of the mineral chemistry of ultramafic xenoliths from the Panshishan area of Jiangsu province are listed in tables 1–4.

Based on classification norms proposed by Menzies (1983), the ultramafic xenoliths in the present study belong to type-I xenoliths. The Fo-values in olivine of the ultramafic xenoliths range from 90.18 to 92.18 which indicate that they may be residues formed by successive partial melting of the primary mantle. In the xenoliths, orthopyroxene shows a restricted range in Mg : Fe : Ca ratios varying from $En_{89}Fs_{10}Wo_1$, clinopyroxene ranges from $Wo_{43}En_{53}Fs_4$ to $Wo_{49}En_{47}Fs_4$. According to the classification of Stephens and Dawson (1977), these pyroxenes fall within the field of enstatite and diopside/chrome-diopside. Diopsides are comparably magnesium rich with high Mg/(Mg+Fe) = 90.96–95.04. They are relatively rich in Al_2O_3 (2.14–7.55%), Na_2O (0.32–2.57%), TiO_2 (0.10–0.52%) and Cr_2O_3 (0.69–1.60%) but poor in ΣFeO (1.99–2.86%). Enstatites have ΣFeO contents ranging from 4.88 to 6.36%. The presence of low-Al (2.25–4.65%) and high-Mg# (88.92–95.84) is a typical characteristic of depleted xenoliths (Su *et al.* 2009). The plots of Cr_2O_3 *vs.* TiO_2 for clinopyroxene of ultramafic xenoliths (figure 3) fall within

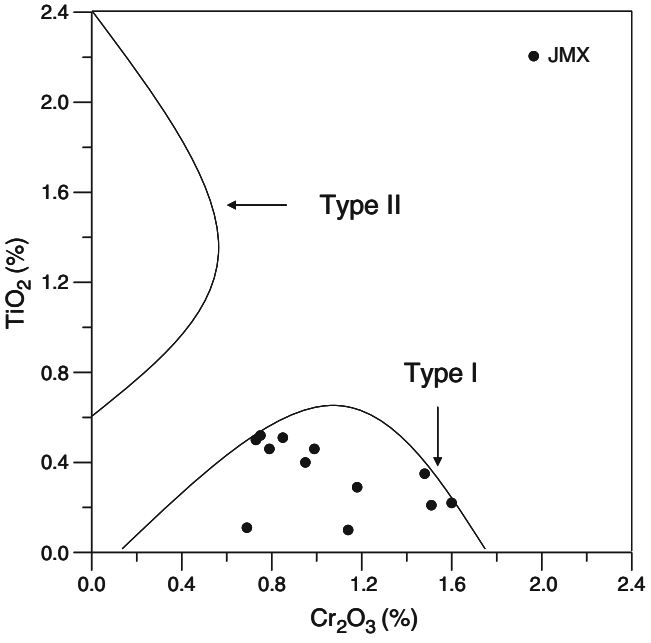

Figure 3. TiO_2 *vs.* Cr_2O_3 plots for clinopyroxene of ultramafic xenoliths from the Jiangsu province. Fields for Type I and Type II from Kempton (1987).

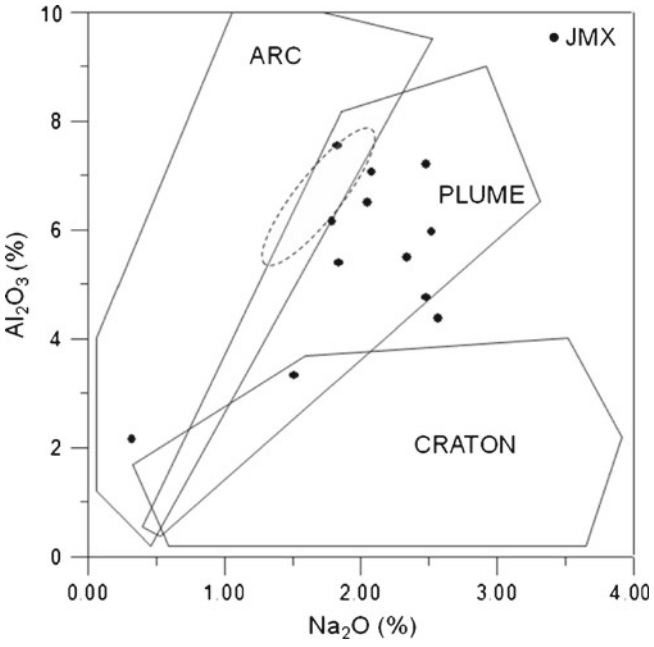

Figure 4. Al_2O_3 *vs.* Na_2O plots for clinopyroxene of ultramafic xenoliths from the Jiangsu province. Fields for ARC, PUUME and CRATON from Kepezhinskas *et al.* (1995). Closed ellipse shows the distribution range of clinopyroxene from southern China (Ho 1998).

type-I xenoliths (Kempton 1987). The Mg# and Cr# in all clinopyroxenes for ultramafic xenoliths from the Panshishan area range from 90.96 to 95.04 and 11.92 to 36.56 which fall within the refractory mantle field (Zheng *et al.* 2003), defined by the Cr# (≥10) and Mg# (≥91). The plots of Al_2O_3 *vs.* Na_2O for clinopyroxene of ultramafic xenoliths (figure 4) fall within the field of plume defined by Kepezhinskas *et al.* (1995).

The spinels have characteristically moderate to high Cr_2O_3 contents (9.46 ∼ 35.89%) and low Al_2O_3 (32.77 ∼ 58.98%) and fall with the range of Cr-spinel and Al-spinel. The Cr/(Cr + Al) ratios of spinel of sample JMX1, JMX2, JMX3 and JMX11 are higher than 50.

5. Bulk chemistry of ultramafic xenoliths

The results of the bulk chemistry of ultramafic xenoliths from the Panshishan area of Jiangsu province are listed in tables 5 and 6. The SiO_2, MgO and ΣFeO contents of the ultramafic xenoliths ranging from 41.12%–44.68%, 38.09%–43.39% and 7.59%–9.09%, respectively. The contents of major elements of ultramafic xenoliths display limited variations. The ultramafic xenoliths have higher MgO content, but lower Al_2O_3, TiO_2, CaO and Na_2O contents than those of primitive mantle proposed by Sun and McDonough (1989).

Table 5. *The major element compositions of ultramafic xenoliths from the Panshishan area, Jiangsu province.*

	JMX1	JMX2	JMX3	JMX4	JMX5	JMX6	JMX7	JMX8	JMX9	JMX10	JMX11	JMX12	P.M.
SiO_2 (%)	41.12	42.78	43.63	44.56	44.66	44.38	43.89	43.66	44.20	44.68	43.32	42.75	44.80
TiO_2	0.035	0.040	0.073	0.104	0.102	0.086	0.071	0.021	0.103	0.123	0.053	0.072	0.210
Al_2O_3	1.39	0.82	1.52	2.49	2.39	2.14	1.98	1.29	2.76	2.87	1.29	2.31	4.45
Cr_2O_3	1.163	0.223	0.406	0.235	0.25	0.267	0.279	0.302	0.317	0.283	0.466	0.319	0.440
ΣFeO	9.09	7.93	7.87	8.58	8.99	8.59	8.70	8.60	8.56	8.12	7.59	8.37	8.40
NiO	0.200	0.201	0.364	0.211	0.203	0.364	0.24	0.264	0.229	0.221	0.27	0.245	0.240
MnO	0.121	0.104	0.100	0.114	0.116	0.111	0.113	0.107	0.115	0.111	0.097	0.112	0.140
MgO	43.39	44.28	42.84	38.09	39.33	39.05	40.54	41.78	39.12	38.16	43.35	41.08	37.20
CaO	0.80	1.54	1.30	2.68	2.38	2.45	1.65	1.41	2.24	3.21	1.21	2.01	3.60
Na_2O	0.135	0.05	0.17	0.189	0.133	0.15	0.134	0.107	0.187	0.175	0.079	0.134	0.340
K_2O	0.042	0.02	0.073	0.011	0.021	0.028	0.041	0.027	0.015	0.030	0.043	0.014	0.030
P_2O_5	0.016	0.06	0.108	0.053	0.023	0.053	0.026	0.043	0.033	0.018	0.078	0.032	0.020
L.O.I.	1.688	2.32	2.254	2.264	1.458	2.271	1.932	2.213	1.793	1.740	2.199	2.223	–
Total	99.190	100.374	100.708	99.581	100.060	99.940	99.596	99.824	99.672	99.741	100.045	99.671	99.870
MgO/ΣFeO	4.77	5.58	5.44	4.44	4.37	4.55	4.66	4.86	4.57	4.70	5.71	4.91	4.43

P.M.: Primitive Mantle (Sun and McDonough 1989).

Table 6. *The trace element compositions of ultramafic xenoliths from the Panshishan area, Jiangsu province.*

	JMX1	JMX2	JMX3	JMX4	JMX5	JMX6	JMX7	JMX8	JMX9	JMX10	JMX11	JMX12
Ba (ppm)	23.51	12.83	23.85	13.06	20.73	14.01	11.43	17.85	11.41	12.27	17.03	13.46
Co	111.5	105.6	92.2	87.8	88.3	91.5	96.1	98.7	92.5	85.7	93.7	92.3
Cu	12.10	9.76	12.25	29.68	24.82	23.39	17.99	9.67	20.65	46.03	10.61	33.52
Hf	0.54	0.11	0.56	0.60	0.23	0.20	0.23	0.15	0.53	0.24	0.29	0.60
Li	4.29	2.74	4.59	3.14	2.80	3.82	3.17	3.33	2.78	3.41	3.67	2.88
Nb	4.78	1.43	3.78	0.67	0.19	0.98	0.26	0.32	0.11	0.54	2.75	2.39
Pb	1.04	9.14	1.80	0.88	2.73	3.22	0.90	1.60	1.18	4.26	2.08	2.09
Rb	1.19	0.89	1.75	0.84	0.78	0.77	1.71	1.28	0.70	1.28	1.40	0.90
Sc	11.26	4.61	8.86	14.05	11.28	11.08	9.82	8.71	14.46	13.77	7.08	11.40
Sr	11.84	46.55	46.17	24.79	11.57	30.81	12.32	11.82	9.10	19.34	40.36	20.63
Th	0.13	0.14	0.24	0.07	0.04	0.13	0.04	0.06	0.03	0.05	0.22	0.05
U	0.11	0.08	0.16	0.06	0.04	0.10	0.04	0.05	0.05	0.05	0.13	0.07
V	32.16	10.16	18.79	44.88	43.88	44.22	32.78	27.525	50.85	56.79	14.27	34.79
Y	0.48	0.66	1.11	2.31	2.37	2.01	1.56	0.576	2.49	3.29	0.87	1.66
Zn	50.45	33.18	41.09	23.70	28.64	32.79	22.80	25.02	22.22	26.23	23.04	24.54
Zr	21.64	5.12	25.23	26.64	9.47	10.04	9.19	6.99	21.23	8.13	11.45	25.58
La	0.741	1.430	2.440	0.398	0.317	1.648	0.536	0.579	0.186	0.705	2.125	0.143
Ce	2.05	3.36	5.67	1.21	1.07	4.82	1.48	1.41	0.80	2.56	4.84	0.61
Nd	0.58	0.75	1.42	0.52	0.48	1.70	0.53	0.36	0.46	1.09	1.16	0.34
Sm	0.148	0.199	0.358	0.202	0.243	0.474	0.170	0.091	0.219	0.403	0.275	0.131
Eu	0.042	0.044	0.087	0.076	0.074	0.135	0.056	0.024	0.077	0.123	0.066	0.051
Gd	0.120	0.153	0.292	0.265	0.286	0.428	0.194	0.072	0.262	0.443	0.229	0.194
Tb	0.014	0.022	0.037	0.050	0.052	0.058	0.034	0.011	0.055	0.074	0.030	0.034
Yb	0.274	0.060	0.103	0.230	0.255	0.170	0.187	0.078	0.272	0.356	0.073	0.176
Lu	0.009	0.011	0.014	0.044	0.039	0.029	0.030	0.014	0.044	0.053	0.013	0.031

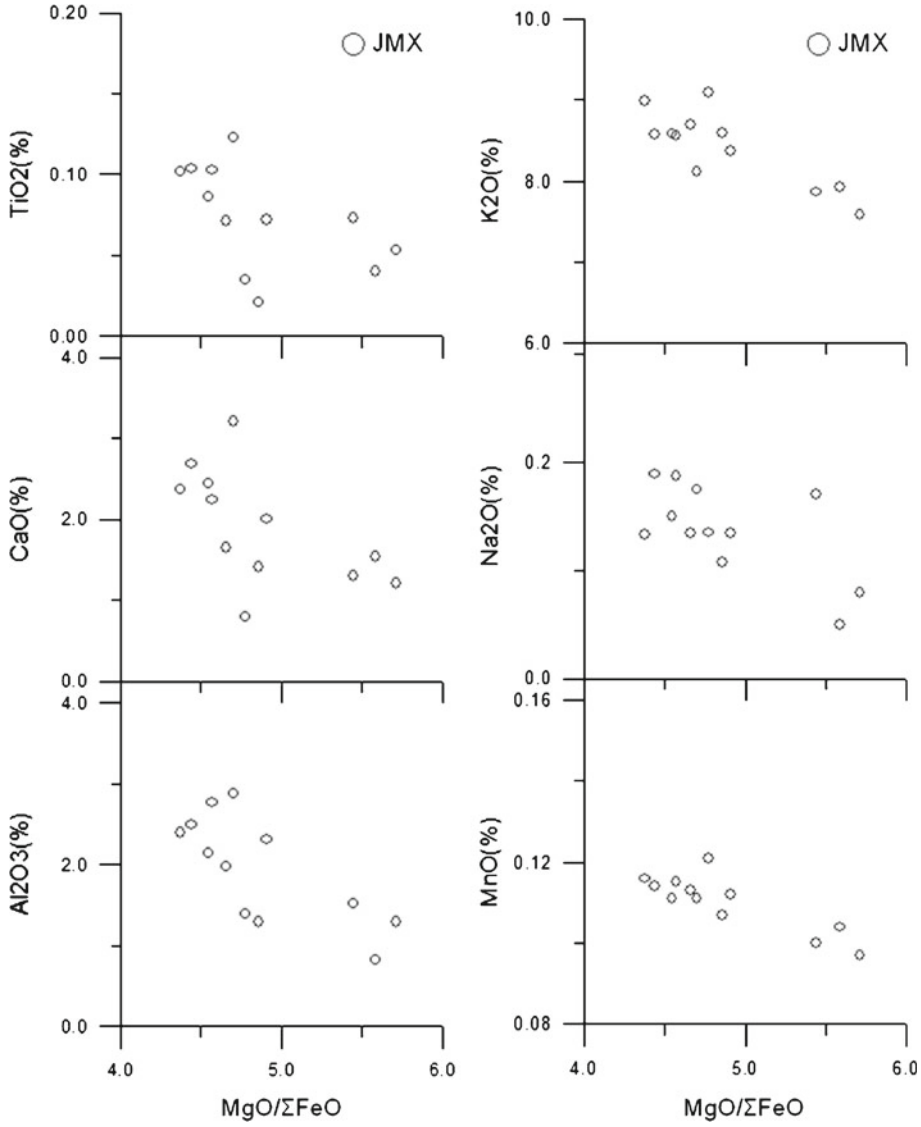

Figure 5. Major elements *vs.* MgO/ΣFeO ratio plots for ultramafic xenoliths from Jiangsu province.

In the Panshishan ultramafic xenoliths, Al_2O_3, TiO_2, CaO, K_2O, Na_2O and MnO tend to decrease with increasing MgO/ΣFeO ratios (figure 5). The chemical variation may be related to the partial melting of the mantle source which removed the elements mentioned above.

The abundance of Sr, Th, Rb, U and Nb are positively correlated with MgO/ΣFeO ratios of the ultramafic xenoliths (figure 6). Except for samples JMX5, JMX9 and JMX12, the chondrite-normalized rare earth element (REE) patterns of the ultramafic xenoliths from the Panshishan area (figure 7) show moderate sloping with light rare earth element (LREE) enrichment. The samples JMX2, JMX3 and JMX11 are decuple higher in light rare elements when compared with chondrete. The $(La/Yb)_N$ ratios of the samples JMX5, JMX9 and JMX12 are 0.89, 0.49, 0.58, respectively. It should be noted that the spinel-therzolite xenoliths can be divided into two types in the Panshishan area: (1) an E-type enriched in LREE with $(La/Yb)_N$ ratios varying from 1.24 to 20.90; (2) a D-type depleted in LREE with $(La/Yb)_N$ ratios varying from 0.49 to 0.89 (such as samples JMX5, JMX9 and JMX12). The isotopic ratios of the ultramafic xenoliths in the Panshishan area are $^{87}Sr/^{86}Sr = 0.702907–0.704349$ and $^{143}Nd/^{144}Nd = 0.512683–0.513371$ (table 7, figure 8). In the primitive mantle normalized incompatible element pattern (figure 9), the ultramafic xenoliths found in Jiangsu province are enriched in Rb, Ba, U, Nb, K, La, Ce, Sr, P and Zr contents which may be related to the CO_2–H_2O-fluids metasomatism. The Th, Ti and Nd depletions in the Panshishan ultramafic xenoliths may be related to the partial melting of the mantle source.

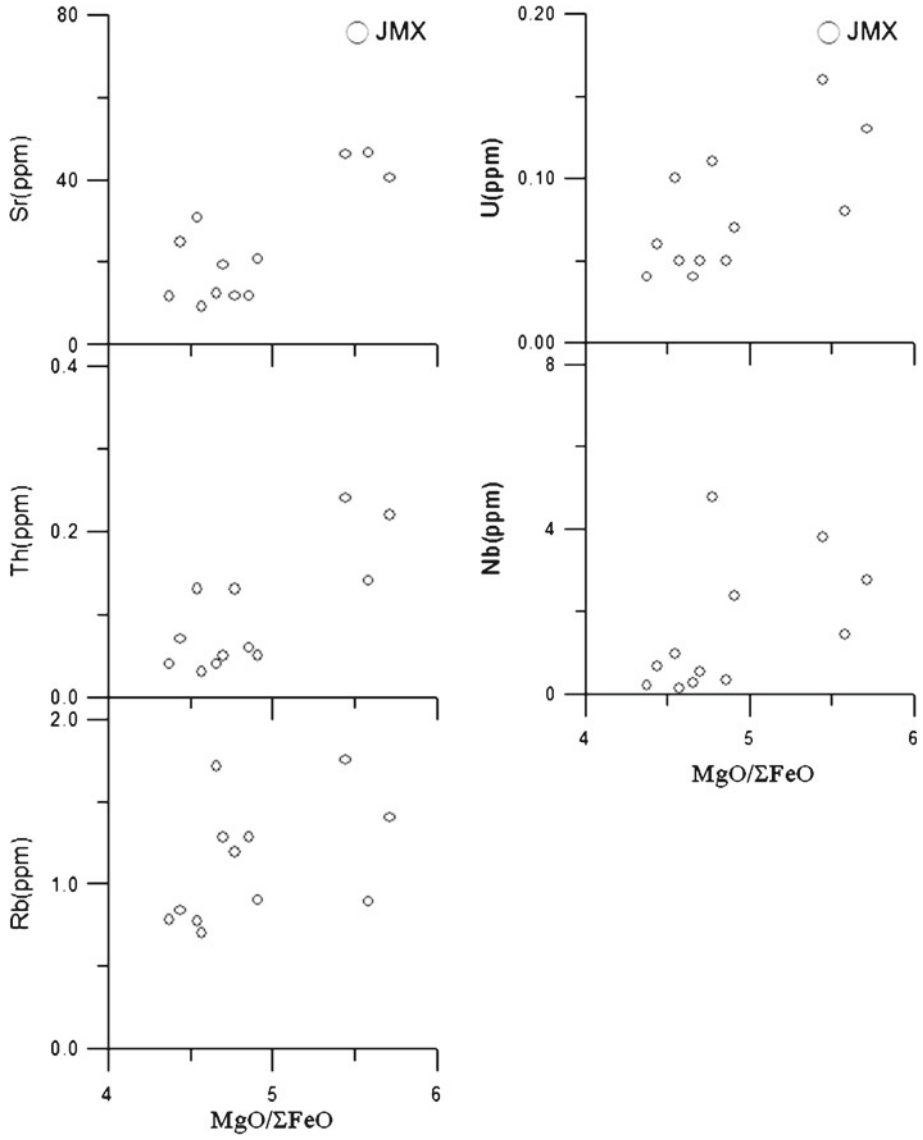

Figure 6. Sr, Th, Rb, U, and Nb *vs.* MgO/ΣFeO ratio plots for ultramafic xenoliths from Jiangsu province.

6. Discussion

6.1 *Geochemical characteristics and genesis of the ultramafic xenoliths in the Panshishan area and their geological implication*

The Panshishan ultramafic xenoliths belong to type I xenoliths and have high Fo-values in olivine which indicate that the ultramafic xenoliths may represent the residues of partial melting. The Mg# and Cr# in all clinopyroxenes for ultramafic xenoliths from the Panshishan area suggested that an old refractory mantle beneath the Panshishan region. The plots of Al_2O_3 *vs.* Na_2O for clinopyroxene of ultramafic xenoliths (figure 4) suggested that the mantle source beneath the study area may be similar to clinopyroxene of mantle source related to subduction (Condie *et al.* 2004). Xia *et al.* (2013) pointed out the ENCC experienced widespread lithospheric thinning from a thick (~200 km), cold (~40 mW/m^2) and highly refractory lithospheric mantle in the mid-Ordovician to a hot (60–80 mW/m^2), thin (60–80 km) and fertile lithospheric mantle since the late Mesozoic.

The major element contents *vs.* MgO/ΣFeO ratios of the ultramafic xenoliths indicate that they may represent residues formed by different degrees of partial melting from the upper mantle. The positive correlation between some trace element contents and MgO/ΣFeO ratios (figure 6) provides support for the suggestion that mantle metasomatism occurred in the Panshishan area. According to mantle xenoliths (Tatsumoto *et al.* 1992; Fan *et al.* 2000; Chen *et al.* 2001; Xu 2002; Zhou *et al.* 2002; Xu and Bodinier 2004), the Cenozoic lithospheric mantle beneath the NCC is fertile in major oxides and depleted in Sr–Nd–Pb isotopic ratios relative to primitive mantle. The temporal and

spatial variations of Sr–Nd–Pb isotopic compositions of middle Jurassic to late Cretaceous mafic rocks across the Chenzhou-Linwu Fault within the South China Block proposed by Wang *et al.* (2008), suggest that the multiple mantle reservoirs including FOZO-, DMM-, EM1- and EM2-like components exist beneath the South China Block.

The varied $(La/Yb)_N$ ratios in the Panshishan xenoliths may be interpreted as due to mantle heterogeneity beneath the Panshishan region. The Sr–Nd variation in the Panshishan xenoliths may be related to the heterogeneous characteristics in the Panshishan region and the influence of different degrees of fluids-metasomatism on mantle composition. The enrichment of Rb, Ba, U, Nb, K, La, Ce, Sr, P and Zr contents in the Panshishan xenoliths may be caused by the CO_2–H_2O-fluids metasomatism. Our results are consistent with previous studies (e.g., Griffin *et al.* 1992, 1998; Yuan 1996; Fan *et al.* 2000; Xu *et al.* 2000) which revealed that Cenozoic lithospheric mantle of North China Block was characterized by chemically fertile but Sr–Nd isotopically depleted compositions.

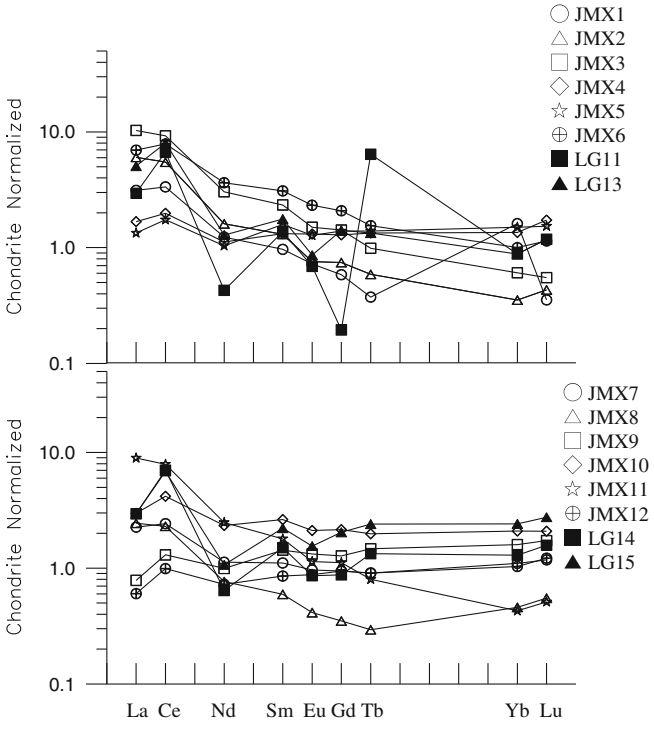

Figure 7. Chondrite-normalized REE patterns of ultramafic xenoliths from Jiangsu province.

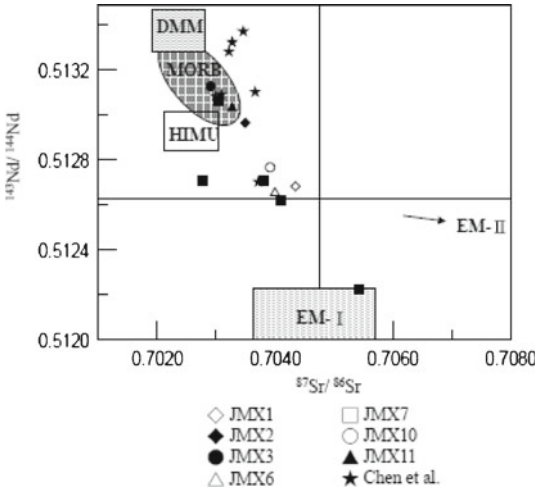

Figure 8. $^{87}Sr/^{86}Sr$ *vs.* $^{143}Nd/^{144}Nd$ plots for ultramafic xenoliths from Jiangsu province (star from Chen *et al.* 1990; closed squares from Dai *et al.* 2008).

Table 7. *The Sr–Nd isotopic data of ultramafic xenoliths from the Panshishan area, Jiangsu province.*

Sample no.	Rock type	$^{87}Sr/^{86}Sr$	$^{143}Nd/^{144}Nd$
JMX1[a]	Spinel-lherzolite	0.703491	0.512965
JMX2[a]	Spinel-lherzolite	0.704349	0.512683
JMX3[a]	Spinel-lherzolite	0.703916	0.512766
JMX6[a]	Spinel-lherzolite	0.703272	0.513035
JMX7[a]	Spinel-lherzolite	0.703050	0.513061
JMX10[a]	Spinel-lherzolite	0.702907	0.513127
JMX11[a]	Spinel-lherzolite	0.703999	0.512659
PS2[b]	Spinel-lherzolite	0.703273	0.513324
PSS1[b]	Spinel-lherzolite	0.702996	0.513083
PSS2[b]	Spinel-lherzolite	0.703089	0.513090
PSS3[b]	Spinel-lherzolite	0.703457	0.513371
PSS6[b]	Spinel-lherzolite	0.703659	0.513102
PSS7[b]	Spinel-lherzolite	0.703218	0.513282
LHFS[b]	Spinel-lherzolite	0.703716	0.512703

Note: [a]Present study. [b]Chen *et al.* (1990).

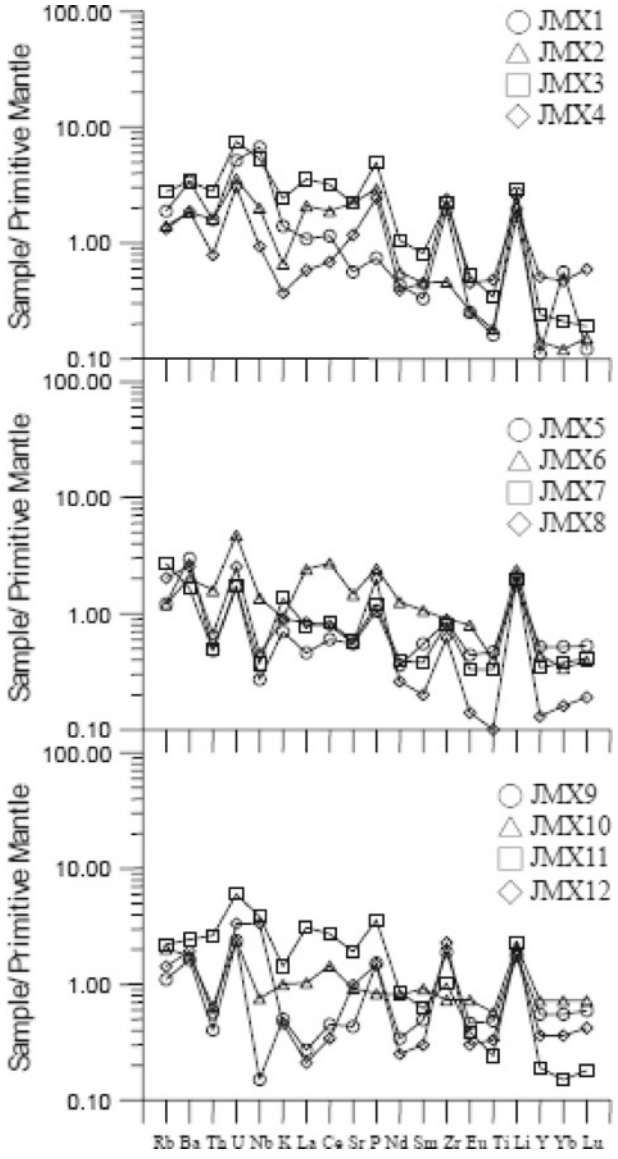

Figure 9. Primitive mantle normalized incompatible element patterns for ultramafic xenoliths from Jiangsu province.

Table 8. *The equilibrium conditions of utramafic xenoliths from the Panshishan area, Jiangsu province.*

	Fabries (1979) Spinel-olivine (°C)	Mysen (1976) Opx-Cpx (°C)	Mysen (1976) Opx-Cpx (kb)
JMX-1	913	920	13
JMX-2	962	916	13
JMX-3	975	1009	19
JMX-4	946	1045	22
JMX-5	893	982	17
JMX-6	976	1016	20
JMX-7	992	1017	20
JMX-8	930	1028	21
JMX-9	948	1009	19
JMX-10	984	990	18
JMX-11	967	1017	20
JMX-12	981	966	16

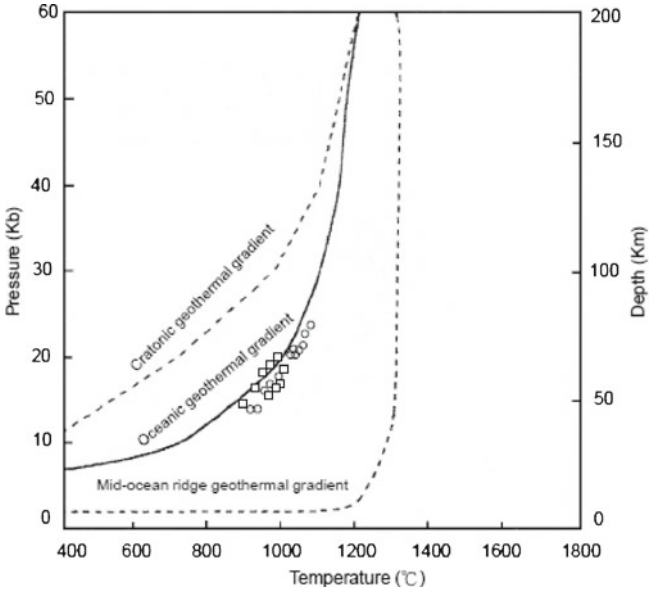

Figure 10. The P–T conditions of the upper mantle beneath the study area (modified after Wyllie 1981; the open circles, this study; open squares from Chen *et al.* 2001).

6.2 *Upper mantle P–T conditions and mantle metasomatism beneath North China Craton (NCC)*

Most xenoliths are useful tools to estimate the pressures and temperatures of formation in terms of available experimental data. These temperature and pressure estimates from ultramafic xenoliths may provide important information on the thermal and dynamic evolution of their lithospheric source regions.

There are many geothermobarometers based on the mineral assemblages of ultramafic rocks, and each geothermometer or geobarometer has its own particular criteria for appropriate use. After reevaluating the geothermobarometers commonly used in the studies of basalt-borne xenoliths, Xu *et al.* (1998) recommended a protocol for pressure and temperature calculation in ultramafic xenoliths. The pressures and temperatures of the lherzolite xenoliths from Jiangsu province were calculated following these protocols. Calculations based on clinopyroxene geothermometry (Mysen 1976) and olivine-spinel geothermometry (Fabries 1979) reveal that the equilibrium conditions of the spinel lherzolite xenoliths in the Panshishan area are: T = 913 ∼ 1045°C, P = 13 ∼ 22 kb corresponding to depths of 45 ∼ 83 km (table 8, figure 10). We incorporate the P–T data from Hannuoba xenoliths, Sino-Korean Craton in figure 10 which suggest that the geothermal gradient of the upper mantle beneath the study area and Hannuoba

area is approximately similar to oceanic geotherm. Tang *et al.* (2006) proposed that continental collision (India–Eurasia collision) and asthenospheric upwelling might be important mechanisms for triggering the melting of asthenospheric material with/without minor component of old lithospheric mantle. Xia *et al.* (2013) suggested that the present NCC lithospheric mantle may be interpreted in terms of relic mantle after the thinning event, while some newly accreted and cooled asthenospheric mantle do exist. The relatively thin crust and lithosphere in eastern China may be caused by mantle upwelling which triggered partial melting of lithospheric mantle (Chung 1999; Deng *et al.* 2004; Lee *et al.* 2006). The geothermal gradient of the upper mantle beneath the study area is suggested that lithospheric mantle thinning accompanied by asthenosphere upwelling has occurred and a newly accreted and cooled asthenospheric mantle may exist beneath the study area. Based on Re-Os studies (Gao *et al.* 2002; Zhi and Qin 2004), ancient lithosphere beneath the Central Zone of the NCC has been documented in mantle xenoliths which do not have low $^{143}Nd/^{144}Nd$ and high $^{87}Sr/^{86}Sr$ ratios (Song and Fery 1989; Rudnick *et al.* 2004; Xu *et al.* 2004).

According to the equilibrium condition for the enriched-type spinel-lherzolite (P = 17.3–32.5 kb) and for the deleted-type spinel-lherzolite (P = 16.3–18.3 kb) Chen *et al.* (2003) suggested that mantle heterogeneity may exist in the Longgang area, Jilin province. Based on major and trace elements and Sr–Nd–Pb isotope data for Cretaceous mafic dikes from the Jiaodong Peninsula, Yang *et al.* (2004) suggested heterogeneous mantle sources may exist beneath the Jiaodong Peninsula.

Xu and Bodinier (2004) reported that metasomatism may have occurred after late Mesozoic lithospheric thinning, which marked a dramatic change in lithospheric architecture beneath the Sino-Korean Craton. The $(La/Yb)_N$ ratios of ultramafic xenoliths in the present study vary from 0.49 to 20.90 indicating mantle heterogeneity in the Panshishan region. The Sr–Nd isotopic composition of this study suggested heterogeneous characteristics in the Panshishan region and the influence of different degrees of fluids-metasomatism on mantle composition (Xia *et al.* 2013). Lee *et al.* (2006) pointed out that basaltic rocks from Shandong province may be derived from partial melting of lithospheric mantle (MORB-like) involved a few EM1 components which may be produced by the recent H_2O–CO_2 fluid metasomatism. H_2O contents of the Cenozoic lithospheric mantle beneath ENCC revealed by mantle xenoliths hosted by alkali basalts (e.g., Penglai, Qixia, Changle, Hebi, Nushan, Panshishan, Lianshan, Fangshan and Beiyan) have been well studied (Yang *et al.* 2008; Bonadiman *et al.* 2009; Xia *et al.* 2010).

The H_2O contents of clinoproxene, orthopyroxene and whole-rock of peridotite xenoliths hosted by the WECC Cenozoic basalts range from 30 to 654 ppm, 14 to 225 ppm and 6 to 262 ppm, respectively (Xia *et al.* 2013). Xia *et al.* (2013) suggested that the H_2O contents of the Cenozoic lithospheric mantle represented by peridotite xenoliths fall in a similar range for both WNCC and ENCC. The lower $^{87}Sr/^{86}Sr$ and $^{143}Nd/^{144}Nd$ ratios, slight LILE enrichment (especially for Rb and Ba) and HFSE depletion observed in the spidergrams (figure 9) suggest that the lithospheric mantle beneath the Panshishan region may have experienced a recent H_2O–CO_2 fluid metasomatism event. The fluids-metasomatism may cause the enrichment of Rb, Ba, U, Nb, K, La, Ce, Sr, P and Zr contents in ultramafic xenoliths from the Panshishan area.

7. Conclusions

According to mineral chemistry and chemical compositions of the ultramafic xenoliths, we suggest that these xenoliths belong to type-I xenoliths consisting of olivine, orthopyroxene, clinopyroxene and spinel. The ultramafic xenoliths have higher MgO content, but lower Al_2O_3, TiO_2, CaO and Na_2O contents than those of primitive mantle proposed by Sun and McDonough (1989), indicating that they may represent residues after different degrees of partial melting from the upper mantle. The Cr/(Cr + Al) ratios of spinel and the Fo-values of olivine provide support for the suggestion mentioned above. The enrichment of Rb, Ba, U, Nb, K, La, Ce, Sr, P and Zr of ultramafic xenoliths found in Jiangsu province may be related to the CO_2–H_2O-fluids metasomatism. The wider variation of $(La/Yb)_N$ ratios and incompatible element contents may be due to mantle heterogeneity and fluid-metasomatism in the Panshishan region. On the basis of Sr–Nd isotopic ratios, we suggest that the lithospheric mantle beneath the study area mostly belongs to depleted-type mantle but with slightly enriched signatures, indicating the heterogeneous characteristics in the mantle source and the influence of different degrees of fluids-metasomatism on the mantle composition. The equilibrium P–T conditions of the spinel lherzolite xenoliths in the study area are: T = 913 ∼ 1045°C, P = 13 ∼ 22 kb corresponding to depths of 45 ∼ 83 km. The P–T conditions suggest that the geothermal gradient of the upper mantle beneath the study area is approximately similar to oceanic geotherm which may be caused by asthenosphere upwelling. We suggested that lithospheric mantle thinning accompanied by asthenosphere upwelling has occurred and

a newly accreted and cooled asthenospheric mantle may exist beneath the study area.

Acknowledgements

The authors would like to thank Dr H J Yang of Department of Earth Sciences, National Cheng Kung University for his kind assistance in Sr and Nd isotopic composition analyses.

References

Bence A E and Albee A L 1968 Empirical correction factors for the electron microanalysis of silicates and oxides; *J. Geol.* **76** 382–403.

Bonadiman C, Hao Y T, Coltorti M, Dallai L, Faccini B, Huang Y and Xia Q K 2009 Water contents in pyroxenes from intraplate lithospheric mantle; *European J. Mineral.* **21** 637–647.

Chen D and Peng Z 1985 K–Ar ages and Pb and Sr isotopic characteristics of Cenozoic volcanic rocks in Shandong, China; *Geochimica* **5** 293–303 (in Chinese).

Chen D G, Chou H T, Yang C T and Wang Y S 1990 Petrogenesis of Cenozoic volcanic rocks and isotopic characteristics of mantle sources in Shandong, Anhwei and Jiangsu provinces. The characteristics and dynamics of upper mantle of China; Seismic Press, Beijing, pp. 124–131 (in Chinese).

Chen S H, O'Reilly S Y, Zhou X H, Griffin W L, Zhang G H, Sun M, Feng J L and Zhang M 2001 Thermal and petrological structure of the lithosphere beneath Hannuoba, Sino-Korean Craton, China: Evidence from xenoliths; *Lithos* **56** 267–301.

Chen J C, Hsu C N and Ho K S 2003 Geochemistry of Cenozoic volcanic rocks and related ultramafic xenoliths from the Jilin and Heilongjiang provinces, northeast China; *J. Asian Earth Sci.* **21** 1069–1084.

Chung S L 1999 Trace element and isotope characteristics of Cenozoic basalts around the Tanlu fault with implications for the eastern plate boundary between north and south China; *J. Geol.* **107** 301–312.

Condie K C, Cox J, O'Reilly S Y, Griffin W L and Kerrich R 2004 Distribution of high field strength and rare earth elements in mantle and lower crustal xenoliths from the southwestern United States: The role of grain-boundary phases; *Geochim. Cosmochim. Acta* **68** 3919–3942.

Dai B Z, Jiang S Y, Jiang Y H, Zhao K D and Liu D Y 2008 Geochronology, geochemistry and Hf–Sr–Nd isotopic compositions of Huziyan mafic xenoliths, southern Hunan Province, south China: Petrogenesis and implications for lower crust evolution; *Lithos* **102** 65–87.

Deng J F, Mo X X, Zhao H L, Wu Z X, Luo Z H and Su S G 2004 A new model for the dynamic evolution of Chinese lithosphere: Continental roots-plume tectonics; *Earth-Sci. Rev.* **65** 223–275.

Dostal J, Zhi X C, Muehlenbachs K, Dupuy C and Zhai M Z 1991 Geochemistry of Cenozoic alkali basaltic lavas from Shandong Province, eastern China; *Geochem. J.* **25** 1–16.

Fabries J 1979 Spinel-olivine geothermometry in periodtites from ultramafic complexes; *Contrib. Mineral. Petrol.* **69** 329–336.

Fan W M, Zhang H F, Baker J, Jarvis K E, Mason P R D and Menzies M A 2000 On and off the North China Craton: Where is the Archaean keel? *J. Petrol.* **41** 933–950.

Gao S, Rudnick R L, Carlson R W, Mcdonough W F and Liu Y S 2002 Re–Os evidence for replacement of ancient mantle lithosphere beneath the North China Craton; *Earth Planet. Sci. Lett.* **198** 307–322.

Griffin W L, O'Reilly S Y and Ryan C G 1992 Composition and thermal structure of the lithosphere beneath south Africa, Siberia and China: Proton microscope studies; Int. Symp. on Cenozoic volcanic rocks and deep-seated xenoliths in China and its environ (Beijing, September 8–10, 1992). Abstr., pp. 65–66.

Griffin W L, Zhang A D, O'Reilly S Y and Ryan C G 1998 Phanerozoic evolution of the lithosphere beneath the Sino-Korean Craton; In: *Mantle Dynamics and Plate Interactions in East Asia* (eds) Flower M F J, Chung S L, Lo C H and Lee T Y, *Am. Geophys. Union Geodyn. Ser.* **27** 107–126.

Guo F, Fan W, Wang Y and Lin G 2003 Geochemistry of late Mesozoic mafic magmatism in west Shandong Province, eastern China: Characterizing the lost lithospheric mantle beneath the North China Block; *Geochem. J.* **37** 63–77.

Ho K S 1998 Petrology and geochemistry of Cenozoic basalts from southern China; *Ph.D. thesis*, 580p. (in Chinese).

Huang X L, Xu Y G and Liu D Y 2004 Geochronology, petrology and geochemistry of the granulite xenolith from Nushan, east China: Implication for a heterogeneous lower crust beneath the Sino-Korean Craton; *Geochim. Cosmochim. Acta* **68** 127–149.

Jahn B M 1990 Origin of granulites: Geochemical constraints from archean granulite facies rocks of the Sino-Korean craton, China; In: *Granulites and Crustal Evolution* (eds) Vielzeuf D and Ph Vidal (Netherlands: Kluwer Academic Publishers), pp. 471–492.

Jahn B M, Auvray B, Cornichet J, Bai Y L, Shen Q H and Liu D Y 1987 3.5 Ga old amphibolites from eastern Hebei province, China: Field occurrence, petrography, Sm-Nd isochron age and REE geochemistry; *Precamb. Res.* **34** 311–346.

Kempton P D 1987 Mineralogic and geochemical evidence for differing styles of metasomatism in spinel lherzolite xenoliths: Enriched mantle source regions of basalts; In: *Mantle Metasomatism* (eds) Menzies M and Hawkesworth C J (New York: Academic Press), pp. 45–89.

Kepezhinskas P K, Defant M J and Drummond M S 1995 Sodium metasomatism in the island arc mantle by slab meltperidotite interaction; *J. Petrol.* **36** 1505–1527.

Lee Y T, Chen J C, Shih J Y, Juang W S, Yang H R, Huang S W and Lin M L 2006 Geochemistry of Cenozoic basaltic rocks from Shandong province and its implication for mantle process in North China; *Geochem. J.* **40** 579–596.

Li Z X 1994 Collision between the North and South China blocks: A crustal-detachment model for suturing in the region east of the Tanlu fault; *Geology* **22** 739–742.

Liu R X, Chen W J, Sun J Z and Li D M 1992 The K–Ar age and tectonic environment of Cenozoic volcanic rocks in China; In: *The Age and Geochemistry of Cenozoic Volcanic Rocks in China* (ed.) Liu R X (Beijing: Seismology Publication), pp. 1–43 (in Chinese).

Menzies M A 1983 Mantle ultramafic xenoliths in alkaline magmas: Evidence for mantle heterogeneity modified by magmatac activity; In: *Continental Basalts and Mantle Xenoliths* (eds) Hawkesworth C J and Norry M J (London: Shiva Publ.), pp. 92–110.

Menzies M A, Fan W M and Zhang M 1993 Paleozoic and Cenozoic lithoprobes and the loss of >120 km of Archean lithosphere, Sino-Korean Craton, China; In: *Magmatic Processes and Plate Tectonics* (eds) Prichard H M, Alabaster T, Harris N B W and Neary C R, *Geol. Soc. London Spec. Publ.* **76** 71–81.

Menzies M A and Xu X 1998 Geodynamics of the North China Craton; In: *Mantle Dynamics and Plate Interactions in East Asia* (eds) Flower M F J, Chung S L, Lo C H and Lee T Y, *Am. Geophys. Union Geodyn. Ser.* **27** 167–195.

Mysen B O 1976 Experimental determination of some geochemical parameters relating to conditions of equilibration of periodtite in the upper mantle; *Am. Mineral.* **61** 677–683.

Okay A I and Sengör A M C 1992 Evidence for intracontinental thrust-related exhumation of the ultra-high-pressure rocks in China; *Geology* **20** 411–414.

O'Reilly S Y, Griffin W L, Poudjom Y H, Morgan P 2001 Are lithosphere forever? Tracking changes in subcontinental lithospheric mantle though time; *GSA Today* **11** 4–10.

Rudnick R L, Gao S, Ling W L, Liu Y S and Mcdonough W F 2004 Petrology and geochemistry of spinel peridotite xenoliths from Hannuoba and Qixia, North China Craton; *Lithos* **77** 609–637.

Smith A D and Huang L Y 1997 The use of extraction chromatographic materials in procedures for the isotopic analysis of neodymium and strontium in rocks by thermal ionisation mass spectrometry; *J. National Cheng-Kung University* **32** 1–10.

Song Y and Fery F A 1989 Geochemistry of peridotite xenoliths in basalt from Hannuoba, eastern China: Implications for subcontinental mantle heterogeneity; *Geochim. Cosmochim. Acta* **53** 97–113.

Stephens W E and Dawson J B 1977 Statistical comparison between pyroxenes from kimberlities and their associated xenoliths; *J. Geol.* **85** 433–449.

Su B X, Zhang H F, Ying J F, Xiao Y and Zhao X M 2009 Nature and processes of the lithospheric mantle beneath the western Qinling: Evidence from deformed peridotitic xenoliths in Ceenozoic kamafugite from Haoti, Gansu Province, China; *J. Asian Earth Sci.* **34** 258–274.

Sun S S and McDonough W F 1989 Chemical and isotopic systematics of oceanic basalts: Implications for mantle composition and processes; *J. Geol. Soc. London Spec. Publ.* **42** 313–345.

Tang Y J, Zhang H F and Ying J F 2006 Asthenosphere–lithospheric mantle interaction in an extensional regime: Implication from the geochemistry of Cenozoic basalts from Taihang Mountains, North China Craton; *Chem. Geol.* **233** 309–327.

Tatsumoto M, Basu A R, Huang W K, Wang J W and Xie G H 1992 Sr, Nd, and Pb isotopes of ultramafic xenoliths in volcanic rocks of eastern China: Enriched components EMI and EMII in subcontinental lithosphere; *Earth Planet. Sci. Lett.* **113** 107–128.

Wang Y, Fan W, Gawood P A and Li S 2008 Sr–Nd–Pb isotopic constraints on multiple domains for Mesozoic mafic rocks beneath the South China Block hinterland; *Lithos* **106** 297–308.

Wilde S A, Zhou X, Nemchin A A and Sun M 2003 Mesozoic crust–mantle interaction beneath the North China Craton: A consequence of the dispersal of Gondwanaland and accretion of Asia; *Geology* **31** 817–820.

Wyllie P J 1981 Plate tectonics and magma genesis; *Geol. Rundsch.* **70** 128–153.

Xia Q K, Hao Y T, Li P, Deloule E, Coltorti M, Dallai L, Yang X Z and Feng M 2010 Low water contents of the Cenozoic lithospheric mantle beneath the eastern part of the North China Craton; *J. Geophys. Res.* **115** B07207, doi: 10.1029/2009JB006694.

Xia Q K, Hao Y T, Liu S C, Gu X Y and Feng M 2013 Water contents of the Cenozoic lithospheric mantle beneath the western part of the North China Craton: Peridotite xenoliths constraints; *Gondwana Res.* **23(1)** 108–118.

Xu J W 1993 *The Tangcheng–Lujiang Wrench Fault System* (New York; Wiley), 279p.

Xu J and Zhu G 1994 Tectonic models of the Tan-Lu fault zone, eastern China; *Int. Geol. Rev.* **36** 771–784.

Xu Y G 2001 Thermo-tectonic destruction of the Archaean lithospheric keel beneath eastern China: Evidence, timing and mechanism; *Physics and Chemistry of the Earth(A)* **26** 747–757.

Xu Y G 2002 Evidence for crustal components in the mantle and constrains on crustal recycling mechanisms: Pyroxenite xenoliths from Hannuoba, North China; *Chem. Geol.* **182** 301–322.

Xu J W, Zhu G, Tong W, Cui K and Liu Q 1987 Formation and evolution of the Tangcheng–Lujiang wrench fault system: A major shear system to the northeast of the Pacific Ocean; *Tectonophys.* **134** 273–310.

Xu X, O'Reilly S Y, Zhou X and Griffin W L 1998 The nature of the Cenozoic lithosphere at Nushan, eastern China; In: *Mantle Dynamics and Plate Interactions in East Asia* (eds) Flower M F J, Chung S L, Lo C H and Lee T Y, *Am. Geophys. Union Geodyn. Ser.* **27** 167–195.

Xu X S, O'Reilly S Y, Griffin W L and Zhou X 2000 Genesis of young lithospheric mantle in southeastern China: An LAM-ICPMS trace element study; *J. Petrol.* **41** 111–148.

Xu Y G and Bodinier J-L 2004 Contrasting enrichments in high and low temperature xenoliths from Nushan, Eastern China: Results of a single metasomatic event during lithospheric accretion? *J. Petrol.* **45** 321–341.

Xu Y G, Chung S L, Ma J and Shi L 2004 Contrasting Cenozoic lithospheric evolution and architecture in the western and eastern Sino-Korean craton: Constraints from geochemistry of basalts and mantle xenoliths; *J. Geol.* **112** 593–605.

Yang J H, Chung S L, Zhai M G and Zhou X H 2004 Geochemical and Sr–Nd–Pb isotopic compositions of mafic dikes from the Jiaodong Peninsula, China: Evidence for vein-plus-peridotite melting in the lithospheric mantle; *Lithos* **73** 145–160.

Yang X Z, Xia Q K, Deloule E, Dallai L, Fan Q C and Feng M 2008 Water in minerals of continental lithospheric mantle and overlying lower crust: A comparative study of peridotite and granulite xenoliths from the North China Craton; *Chem. Geol.* **256** 33–45.

Yin A and Nie S Y 1993 An indentation model for the north and south China collision and the development of the Tan-lu and Honam fault systems, eastern Asia; *Tectonics* **12** 801–813.

Ying J F, Zhang H F, Kita N, Morishita Y and Shimoda G 2006 Nature and evolution of Late Cretaceous lithospheric mantle beneath the eastern North China Craton: Constraints from petrology and geochemistry of peridotitic xenoliths from Jünan, Shandong Province, China; *Earth Planet. Sci. Lett.* **244** 622–638.

Yuan X 1996 Velocity structure of Qinling lithosphere and mushroom cloud model; *Sci. China, Ser. D* **39** 235–244.

Zhang H F 2005 Transformation of lithospheric mantle through peridotite-melt reaction: A case of Sino-Korean Craton; *Earth Planet. Sci. Lett.* **237** 768–780.

Zhang M, Zhou X H and Zhang J B 1998 Nature of the lithospheric mantle beneath NE China: Evidence from potassic volcanic rocks and mantle xenoliths; In: *Mantle Dynamics and Plate Interactions in East Asia* (eds) Flower M F J, Chung S L, Lo C H and

Lee T Y, *Geodynamics Series*, AGU, Washington **27** 197–219.

Zhang H H, Xu Y G, Ge W C and Ma J L 2006 Geochemistry of late Mesozoic–Cenozoic basalts in Yitong–Datun area. Jilin Province and its implication; *Acta Petrologica Sinica* **22** 1579–1607.

Zhao D 2001 Seismic structure and origin of hotspots and mantle plumes; *Earth Planet. Sci. Lett.* **192** 251–265.

Zheng Y F, Fu B, Gong B, Feng W M, Li L and Li Y L 2003 Stable isotope geochemistry of ultrahigh pressure metamorphic rocks from the Dabie-Sulu orogenic belt: Implications for geodynamics and fluid regimes; *Earth Sci. Rev.* **62** 105–161.

Zhi X C and Qin X 2004 Re–Os isotope geochemistry of mantle derived peridotite xenoliths from eastern China: Constraints on the age and thinning of lithosphere mantle; *Acta Petrol. Sin.* **20** 989–998 (in Chinese with English abstract).

Zhou X H, Sun M, Zhang G H and Chen S H 2002 Continental crust and lithospheric mantle interaction beneath north China: Isotopic evidence from granulite xenoliths in Hannuoba, Sino-Korean craton; *Lithos* **62** 111–124.

Zou H B, Zindler A, Xu X S and Qi Q 2000 Major, trace element, and Nd, Sr and Pb isotope studies of Cenozoic basalts in SE China: Mantle sources, regional variations, and tectonic significance; *Chem. Geol.* **171** 33–47.

MS received 2 September 2012; revised 6 January 2013; accepted 13 January 2013